

E7-2022-49

A. V. Isaev\* et al.

FINE STRUCTURE OF THE PROMPT  
NEUTRON MULTIPLICITY DISTRIBUTION  
IN THE SPONTANEOUS FISSION  
OF SUPERHEAVY NUCLEUS  $^{256}\text{Rf}$

Submitted to "Physics Letters B"

---

\* E-mail: isaev@jinr.ru

Исаев А. В. и др.

E7-2022-49

Тонкая структура распределения множественности мгновенных нейтронов спонтанного деления сверхтяжелого ядра  $^{256}\text{Rf}$

Исследование спонтанного деления  $^{256}\text{Rf}$ , синтезируемого в реакции полного слияния  $^{50}\text{Ti} + ^{208}\text{Pb}$ , выполнено на сепараторе SHELS (ЛЯР ОИЯИ). Получено распределение мгновенных нейтронов по множественностям ( $\bar{\nu} = 4,30 \pm 0,17$  и  $\sigma_{\nu}^2 = 3,2$ ). Для изотопа также определены период полураспада  $T_{1/2} = (6,7 \pm 0,2)$  мс и коэффициент ветвления по пути  $\alpha$ -распада  $b_{\alpha} = 0,003^{+0,005}_{-0,003}$ . Детектирующая система сепаратора впервые позволила измерить выходы мгновенных нейтронов для ядра из области сверхтяжелых элементов.

Работа выполнена в Лаборатории ядерных реакций им. Г. Н. Флерова ОИЯИ.

Препринт Объединенного института ядерных исследований. Дубна, 2022

Isaev A. V. et al.

E7-2022-49

Fine Structure of the Prompt Neutron Multiplicity Distribution in the Spontaneous Fission of Superheavy Nucleus  $^{256}\text{Rf}$

An experimental study of  $^{256}\text{Rf}$  spontaneous fission in fusion reaction of  $^{50}\text{Ti} + ^{208}\text{Pb}$  was performed using the velocity filter SHELS (FLNR JINR). The average number of neutrons  $\bar{\nu} = 4.30 \pm 0.17$  and variance  $\sigma_{\nu}^2 = 3.2$  from the prompt neutron multiplicity distribution were obtained. The  $\alpha$ -decay branching ratio  $b_{\alpha} = 0.003^{+0.005}_{-0.003}$  and the half-life  $T_{1/2} = (6.7 \pm 0.2)$  ms of the isotope were determined. For the first time, our neutron detector system allowed us to extend investigation of the prompt neutron multiplicity to the superheavy element region.

The investigation has been performed at the Flerov Laboratory of Nuclear Reactions, JINR.

Preprint of the Joint Institute for Nuclear Research. Dubna, 2022

A. V. Isaev<sup>1</sup>, R. S. Mukhin<sup>1</sup>, A. V. Andreev<sup>1</sup>, M. L. Chelnokov<sup>1</sup>, V. I. Chepigin<sup>1</sup>,  
H. M. Devaraja<sup>1</sup>, O. Dorvaux<sup>2</sup>, B. Gall<sup>2</sup>, K. Hauschild<sup>3</sup>, I. N. Izosimov<sup>1</sup>,  
A. A. Kuznetsova<sup>1</sup>, A. Lopez-Martens<sup>3</sup>, O. N. Malyshev<sup>1,4</sup>, A. G. Popeko<sup>1,4</sup>,  
Yu. A. Popov<sup>1,4</sup>, A. Rahmatinejad<sup>1</sup>, B. Sailaubekov<sup>1,5,6</sup>, T. M. Shneidman<sup>1,7</sup>,  
E. A. Sokol<sup>1</sup>, A. I. Svirikhin<sup>1,4</sup>, M. S. Tezkebayeva<sup>1,5</sup>, A. V. Yeremin<sup>1,4</sup>,  
N. I. Zamyatin<sup>1</sup>

---

<sup>1</sup> Joint Institute for Nuclear Research, Dubna

<sup>2</sup> Université de Strasbourg, CNRS, Strasbourg, France

<sup>3</sup> IJCLab, IN2P3-CNRS, Université Paris-Saclay, Orsay, France

<sup>4</sup> Dubna State University, Dubna, Russia

<sup>5</sup> Institute of Nuclear Physics, Almaty, Kazakhstan

<sup>6</sup> L. N. Gumilyov Eurasian National University, Astana, Kazakhstan

<sup>7</sup> Kazan Federal University, Kazan, Russia

## INTRODUCTION

The paper discusses the search for fission modes using shapes of prompt neutron multiplicity distributions. For the  $^{256}\text{Rf}$  nucleus, bimodal fission can manifest itself in both TKE spectra and the prompt neutron multiplicity distribution. As will be shown below, the prompt neutron multiplicity distributions can have a fine structure and therefore carry valuable information about the mechanism of nuclear fission.

The spontaneous fission process was discovered for uranium in 1940 by G. N. Flerov and K. A. Petrzhak [1]. The energy of the fission reaction is predominantly released as the kinetic energy of the fission fragments. However, a significant part of the energy is also spent on the excitation of fragment nuclei, which can then de-excite by evaporating a certain number of prompt neutrons. The shell structure and deformations of the forming fragments affect the excitation energy, which is reflected in the dependence of the average number of prompt neutrons on the mass number of the fission fragment. This dependence has a “sawtooth” shape with minima, related to magic nuclei [2]. Since the shape of the prompt neutron multiplicity distribution is unique for each isotope, it reveals important information about the fission process. As a consequence, the neutron multiplicity distributions can be used to improve theoretical approaches to nuclear fission. Getting data on neutron yields is especially important and at the same time challenging for short-lived heavy nuclei in the region  $Z \geq 100$ .

Because of the low production rates of the transfermium nuclei, high overall neutron registration efficiency is an essential requirement for any detector system used in online experiments. In this context, the developed efficient neutron detector at the Flerov Laboratory of Nuclear Reactions (FLNR) of JINR [3] made it possible to study the spontaneous fission neutron multiplicities in the transfermium and superheavy regions. The opportunities for studies down to the nanobarn nuclei production cross-section level are achieved.

In the present work, for the first time, a detailed experimental neutron multiplicity distribution study in the region of superheavy nuclei from the spontaneous fission of  $^{256}\text{Rf}$  is presented. The results are discussed along with previously measured nuclei  $^{260}\text{Md}$  and  $^{252}\text{No}$ , as well as together with the calculations of GEF (GENERAL description of Fission observables) [4] and ISP (Improved Scission Point) [5] models.

## 1. EXPERIMENTAL DETAILS

The experiment was carried out at FLNR JINR. The velocity filter SHELS [6] was used to separate the  $^{256}\text{Rf}$  recoils from all other reaction products and the primary beam. The selected  $^{256}\text{Rf}$  recoil will pass through the SHELS separator and time-of-flight (TOF) detectors and, finally, will be implanted into the detection system. The detection system includes 54  $^3\text{He}$ -neutron counters [3] placed around an assembly (“well”-like) of Si detectors [7]. The Si-detector array consists of  $48 \times 48$ -strip focal-plane detector and 4 tunnel 16-strip detectors for fission-fragment and  $\alpha$ -particle registration. The neutron counters allow registering multiple prompt neutrons emitted in the spontaneous fission process of the nucleus (Fig. 1).

The high granularity of the neutron detector enabled us to register multiple neutron events at a time. Consequently, the probability of detecting several neutrons simultaneously in a single  $^3\text{He}$  counter within the coincidence time window is negligible. The neutron registration efficiency, measured with a  $^{248}\text{Cm}$  source is  $(45 \pm 1)\%$ , and the average neutron lifetime in the assembly is  $(23 \pm 1) \mu\text{s}$ . The detection efficiency of the focal-plane Si detector for  $\alpha$  particles emitted by implanted nuclei is  $\sim 50\%$  and  $100\%$  for the detection of at least one of the two fission fragments. Once a fission fragment is detected in the focal-plane DSSD, the signal from the fast output of the spectrometry amplifier triggers the neutron counter circuit interrogation for the duration of  $128 \mu\text{s}$  and the time step of  $1 \mu\text{s}$ .

The complete fusion reaction  $^{208}\text{Pb}(^{50}\text{Ti}, 2n)^{256}\text{Rf}$  was used to synthesize the investigated rutherfordium isotope. The  $^{50}\text{Ti}$  ions were accelerated by the U-400 cyclotron up to the energy of  $(237 \pm 3) \text{ MeV}$ . The PbS target

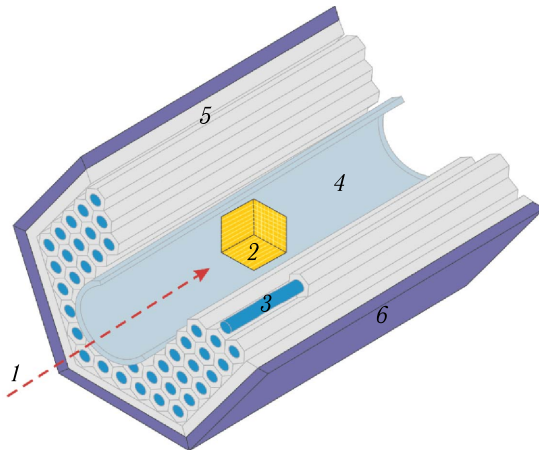


Fig. 1. Cutaway view of the detection system installed at SHELS to investigate neutron multiplicity: 1 — recoil nuclei; 2 — Si-detector array; 3 —  $^3\text{He}$  counters; 4 — vacuum chamber; 5 — moderator; 6 — shield

thickness was  $350 \mu\text{g}/\text{cm}^2$  (the  $^{208}\text{Pb}$  isotope enrichment  $> 99\%$ ), and a  $2\text{-}\mu\text{m}$  thick titanium backing was used. The total number of beam ions that passed through the target and then stopped in a Faraday cup was about  $2.8 \cdot 10^{18}$ .

## 2. RESULTS

Fission fragments from  $^{256}\text{Rf}$  spontaneous fission were searched for the time interval  $0\text{--}62 \text{ ms}$  ( $\sim 10 T_{1/2}$ ) following the registration of the implanted reaction products. A total of 1345  $^{256}\text{Rf}$  spontaneous fissions were found during the data analysis. The  $^{256}\text{Rf}$  half-life was obtained as  $T_{1/2} = (6.7 \pm 0.2) \text{ ms}$  from the time distribution shown in Fig. 2. The value is in good agreement with the previously measured values of  $(6.2 \pm 0.2) \text{ ms}$  [8],  $(6.7 \pm 0.2) \text{ ms}$  [9], and  $(6.9 \pm 0.4) \text{ ms}$  [10].

To determine the  $\alpha$ -decay branching ratio, “recoil- $\alpha_1$ - $\alpha_2$ ” correlations were used. The  $\alpha_1$  was searched for the time interval  $0\text{--}62 \text{ ms}$  from the time of recoil implantation signal, whereas the  $\alpha_2$  was searched for the time interval  $0\text{--}23 \text{ s}$  from the  $\alpha_1$ . Only one correlation was found, where all the  $\alpha$ -decay events are localized in the same pixel of the focal-plane detector ( $^{256}\text{Rf}$ :  $6.015 \text{ ms}$  and  $8714 \text{ keV}$ ;  $^{252}\text{No}$ :  $2.69 \text{ s}$  and  $8373 \text{ keV}$ ). By considering the 25% registration efficiency for our one  $\alpha$ -decay chain event in the focal-plane detector, the  $\alpha$ -decay branching ratio is  $b_\alpha = 0.003^{+0.005}_{-0.003}$ . The obtained  $b_\alpha$  agrees with the previously published value of  $0.0032 \pm 0.0017$  [8].

Prompt neutrons emitted in the spontaneous fission of  $^{256}\text{Rf}$  were searched for the time interval  $0\text{--}128 \mu\text{s}$  from the moment of the fission-fragment registration in the focal-plane DSSD. A total of 2605 prompt neutrons in

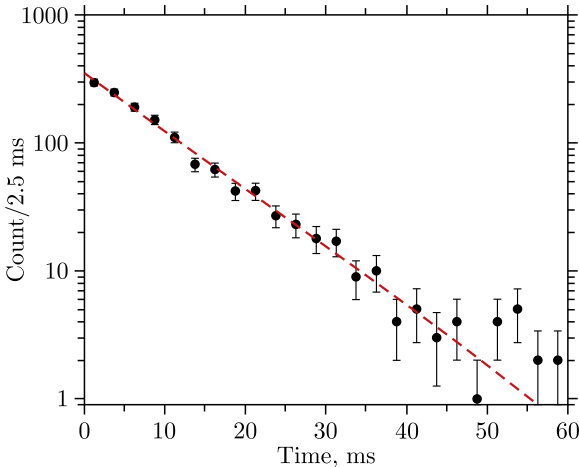


Fig. 2. Distribution of time differences between recoil nuclei and fission-fragment registration for  $^{256}\text{Rf}$ : the symbols represent the experimental data and the dashed line is the fit using the exponential decay function

Table 1. Prompt neutron measured ( $F_n$ ) and emitted ( $P_n$ ) probabilities for  $^{256}\text{Rf}$  spontaneous fission. Here,  $n$  is the neutron multiplicity,  $\Delta F_n$  and  $\Delta P_n$  are the corresponding uncertainties

$n$	$F_n$	$\Delta F_n$	$P_n$	$\Delta P_n$
0	0.148	0.010	0.042	0.014
1	0.259	0.014	0.062	0.018
2	0.255	0.010	0.062	0.021
3	0.215	0.007	0.102	0.021
4	0.096	0.004	0.192	0.022
5	0.024	0.002	0.253	0.022
6	0.002	0.001	0.205	0.019
7	0.001	< 0.001	0.082	0.018
8	0	< 0.001	0	0.014

correlation with 1345  $^{256}\text{Rf}$  spontaneous fission events were registered. The neutron yield data (Table 1) were obtained for the first time. After taking into account the detector efficiency of  $(45 \pm 1)\%$ , the emitted neutron distribution properties were obtained: the mean as  $\bar{\nu} = 4.30 \pm 0.17$  and the variance as  $\sigma_{\nu}^2 = 3.2$ .

The Tikhonov statistical regularization method [11–13] was applied to extract the emission probabilities  $P_n$  from the measured ones  $F_n$ . The reconstruction results are shown in Fig. 3 and presented in Table 1. For the reconstructed distribution, the average number of neutrons is  $4.33 \pm 0.14$  and the variance is 3.3.

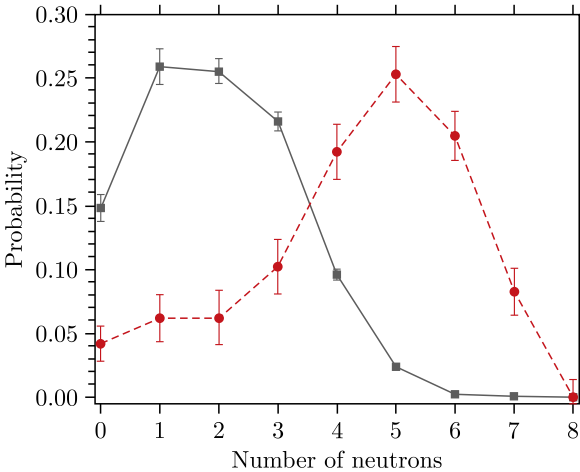


Fig. 3. Probability distributions for the neutrons from the spontaneous fission of  $^{256}\text{Rf}$ : measured in the experiment  $F_n$  (squares) and reconstructed  $P_n$  (circles). The lines have been added to guide the eye

The influence of the background was insignificant in comparison with the level of statistical uncertainties obtained in the experiment (the background-to-signal ratio is less than 1%, whereas the relative statistical uncertainty is about 4%).

### 3. DISCUSSION

The theoretical calculations of neutron multiplicity were carried out within the framework of the ISP model. The details of the model are presented in [5, 14]. In short, the model assumes that after crossing the fission barrier, a fissile nucleus can be described as a superposition of binary systems, specified by the masses, charges, and deformations of its constituent fragments. The potential energy surface is calculated in the mic-mac approach with an accurate account for the shell corrections of the fragments and their damping with excitation energy. The weights of binary systems are determined by their level densities.

The model showed good results for the description of fission observables in the actinide region [15]. In [16], it was realized that to deal with the spontaneous fission of heavier nuclei, the ISP model has to be modified to account for the evolution of the fissile nucleus towards the scission point. It was done by incorporating the additional deformation cut-off function, which ensures that binary systems decay before reaching the configurations with large deformations of the fragments [16].

An attempt to use the same approach for  $^{256}\text{Rf}$  showed that the parameters of the cut-off function cannot be taken in a universal way. Therefore, here we explicitly treat the evolution of the initial distribution of the binary systems as a random walk on the potential energy surface calculated in the ISP model.

The transition probabilities for change of the deformations, masses, and charges of the fragments were evaluated simultaneously with the probability for the binary system to decay in the relative distance (thus undergoing fission). The transition probabilities were taken proportional to the level density of the corresponding final states  $\rho_f(U_f^*)$  to ensure the detailed balance principle between the direct and reverse transitions:  $P_{i \rightarrow f}/P_{f \rightarrow i} = \rho_i(U_i^*)/\rho_f(U_f^*)$ . The level densities  $\rho(U^*)$  are taken in the form of a Fermi gas distribution with the level density parameters depending on the mass number as  $a = A/12$ . For the decay probability, the level density is taken at the top of the barrier in the relative distance.

To determine the initial distribution of the binary systems, we fix the quadrupole moment  $Q_{20}$  of the fissile nucleus to fulfill that, first, the nucleus has already crossed the fission barrier and, second, that there are a significant amount of binary systems with quadrupole moments in the 10% range around  $Q_{20}$ . The value  $Q_{20}$  was fixed to give the best description of the average neutron number in spontaneous fission of  $^{260}\text{Md}$ ,  $^{256}\text{Rf}$  and  $^{252}\text{No}$  nuclei which yield the value of  $Q_{20}$  corresponding to the quadrupole deformation parameter of the fissile nucleus  $\beta_2 = 1.15$ .

The details of the calculations and the application of the model to various nuclei will be presented in the forthcoming publication.

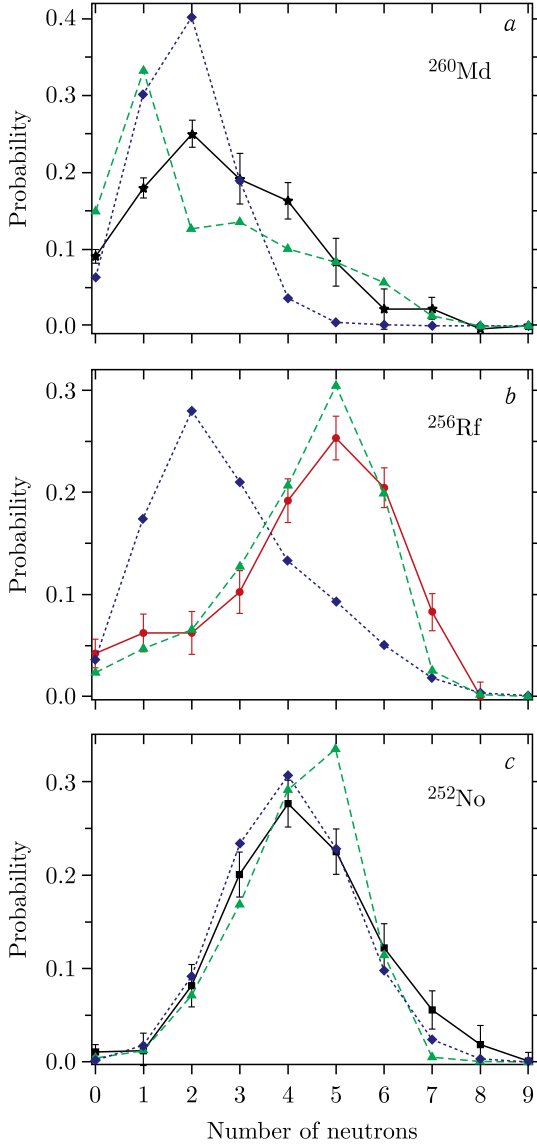


Fig. 4. Prompt neutron emission probability distributions for  $^{260}\text{Md}$  (a),  $^{256}\text{Rf}$  (b), and  $^{252}\text{No}$  (c). Theoretical calculations: triangles — ISP model; rhombuses — GEF model [4]. Experimental data: stars — data from [17]; circles — values obtained in this work; squares — data from [18]. The lines connecting points have been added for clarity

The theoretical calculations were made for  $^{260}\text{Md}$ ,  $^{256}\text{Rf}$ , and  $^{252}\text{No}$ . The  $^{260}\text{Md}$  isotope has a similar to  $^{256}\text{Rf}$  neutron multiplicity distribution behaviour in the region of low neutron multiplicities (described below). At the same time,  $^{252}\text{No}$  is given to show that the behaviour at low neutron multiplicities can differ significantly for other nuclei. For a comparative analysis, the calculations were also carried out with the GEF model [4]. In Fig. 4, the calculation results along with our experimental results are presented. The ISP model predicts the average number of neutrons in the spontaneous fission processes, which agrees with the values measured in experiments for  $^{256}\text{Rf}$  and  $^{252}\text{No}$  nuclei (Table 2). The GEF model underestimates the  $\bar{\nu}$  values for  $^{260}\text{Md}$  and  $^{256}\text{Rf}$ . As regards the shape of the prompt neutron multiplicity distributions, the ISP model provides a better prediction for  $^{256}\text{Rf}$ , while the GEF model predicted well for  $^{252}\text{No}$ .

The experiment shows a significant number ( $\sim 10\%$ ) of  $^{256}\text{Rf}$  spontaneous fission events accompanied by the emission of at most one prompt neutron ( $0n$  and  $1n$  multiplicities). A similar effect (more expressed) was previously observed [17] for  $^{260}\text{Md}$  (Fig. 4), for which bimodal symmetric fission was discovered [19]. This behaviour of the neutron multiplicity distributions of  $^{256}\text{Rf}$  and  $^{260}\text{Md}$  is strikingly different from what we see for  $^{252}\text{No}$  (see Fig. 4).

As shown in [20], the TKE distribution of  $^{256}\text{Rf}$  obtained in experiment contains two components. Two fission modes of  $^{256}\text{Rf}$  were also predicted by theoretical calculations [21], that showed that a high-energy TKE component is characterized by a symmetric mass distribution of fission fragments, while a low-energy TKE component corresponds to an asymmetric mass distribution of fission fragments.

The calculations of TKE distribution and mass distribution of fission fragments were made using the ISP model. The results of calculations are shown in Fig. 5 for various groups of multiplicities of emitted prompt neutrons, as well as for cumulative total contributions. The rise in the left tail of the neutron multiplicity distribution can be explained by the presence of spontaneous fission events for which reaction energy is mainly released in

Table 2. **Comparison of experimental and theoretical prompt neutron multiplicity distributions for  $^{260}\text{Md}$ ,  $^{256}\text{Rf}$ , and  $^{252}\text{No}$**

Isotope	Property	Experiment			Model	
		[17]	This work	[18]	ISP	GEF
$^{260}\text{Md}$	$\bar{\nu}$	$2.58 \pm 0.11$	—	—	2.25	$1.86 \pm 0.04$
	$\sigma_{\nu}^2$	2.6	—	—	3.4	1.0
$^{256}\text{Rf}$	$\bar{\nu}$	—	$4.30 \pm 0.17$	—	4.30	$2.83 \pm 0.12$
	$\sigma_{\nu}^2$	—	3.2	—	2.5	2.6
$^{252}\text{No}$	$\bar{\nu}$	—	—	$4.25 \pm 0.09$	4.22	$4.04 \pm 0.01$
	$\sigma_{\nu}^2$	—	—	2.1	1.4	1.6

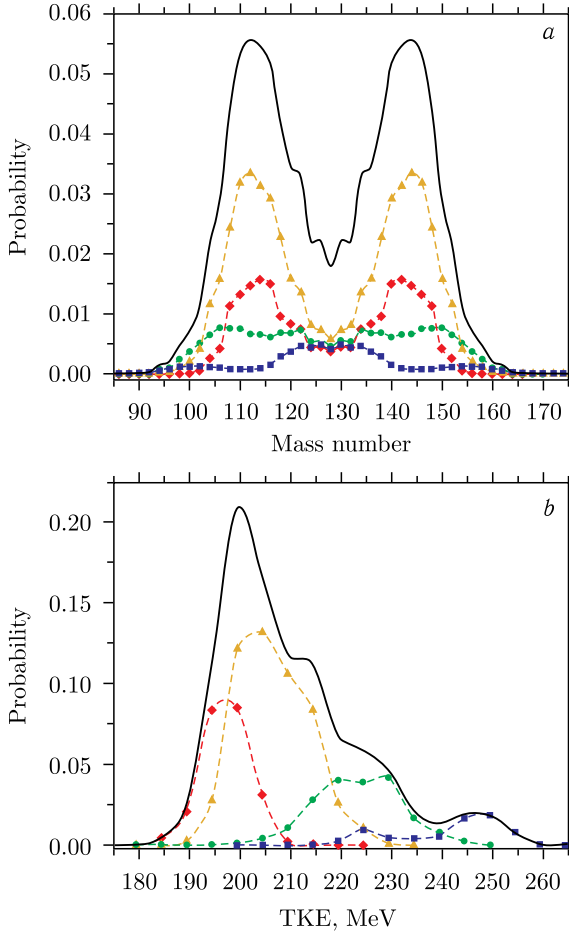


Fig. 5. Calculated mass distributions of fission fragments (*a*) and TKE distributions (*b*) for  $^{256}\text{Rf}$  spontaneous fission. Results are grouped by multiplicities of emitted prompt neutrons: solid line — overall by all multiplicities; squares — from  $0n$  to  $1n$ ; circles — from  $2n$  to  $3n$ ; triangles — from  $4n$  to  $5n$ ; rhombuses — from  $6n$  to  $9n$

the form of the kinetic energy of fission fragments (Fig. 5). Thus, the effect is probably related to the symmetric fission mode of  $^{256}\text{Rf}$ .

## CONCLUSIONS

The prompt neutron emission probabilities of different multiplicities have been observed in the spontaneous fission of  $^{256}\text{Rf}$ . The average number of neutrons in the spontaneous fission process is found to be  $\bar{\nu} = 4.30 \pm 0.17$ , while the variance is  $\sigma_{\nu}^2 = 3.2$ .

The fine structure is revealed in prompt neutron multiplicity distribution of  $^{256}\text{Rf}$ . A rise in the region of low neutron multiplicities, found in the experiment, is most likely associated with the compact fission mode of  $^{256}\text{Rf}$ . This mode is characterized by a large value of the average total kinetic energy and (as a consequence) by a lower neutron evaporation. The ability to see the fine structure in the distributions of prompt neutrons is extremely important for determining fission modes. Especially it concerns spontaneously fissionable nuclei where there are no data on the total kinetic energy and mass distributions of fission fragments.

The experimental results for  $^{256}\text{Rf}$  were compared with predictions made by the ISP model. The agreement found in the average number of neutrons in the spontaneous fission processes and the shape of the model distribution is quite close to the experimental one.

**Acknowledgements.** This work was supported by the Russian Foundation for Basic Research (project No.18-52-15004) and the Joint Institute for Nuclear Research (grant No.22-502-06). T.M.S. was partly supported by the Kazan Federal University Strategic Academic Leadership Program.

## REFERENCES

1. *Flerov G. N., Petrjak K. A.* Spontaneous Fission of Uranium // *Phys. Rev.* 1940. V. 58, No. 1. P. 89; doi:10.1103/PhysRev.58.89.2.
2. *Gindler J.* Dependence of Neutron Yield on Fragment Mass for Several Low-Energy Fissioning Systems // *Phys. Rev. C.* 1979. V. 19, No. 5. P. 1806–1819; doi:10.1103/PhysRevC.19.1806.
3. *Svirikhin A. I. et al.* A Detector for Studying the Characteristics of Spontaneous Fission of Short-Lived Heavy Nuclei // *Instrum. Exp. Tech.* 2011. V. 54, No. 5. P. 644–648; doi:10.1134/S0020441211040154.
4. *Schmidt K.-H. et al.* General Description of Fission Observables: GEF Model Code // *Nucl. Data Sheets.* 2016. V. 131. P. 107–221; doi:10.1016/j.nds.2015.12.009.
5. *Andreev A. V. et al.* Ternary Fission within Statistical Approach // *Eur. Phys. J. A.* 2006. V. 30, No. 3. P. 579–589; doi:10.1140/epja/i2006-10145-2.
6. *Popeko A. G. et al.* Separator for Heavy Element Spectroscopy — Velocity Filter SHELS // *Nucl. Instr. Meth. B.* 2016. V. 376. P. 140–143; doi:10.1016/j.nimb.2016.03.045.
7. *Isaev A. V. et al.* Application of a Double-Sided Stripped Si Detector in the Focal Plane of the VASILISSA Separator // *Instrum. Exp. Tech.* 2011. V. 54, No. 1. P. 37–42; doi:10.1134/S0020441210061028.
8. *Hessberger F. P. et al.* Spontaneous Fission and Alpha-Decay Properties of Neutron Deficient Isotopes  $^{257-253}\text{104}$  and  $^{258}\text{106}$  // *Z. Phys. A: Hadrons Nucl.* 1997. V. 359, No. 4. P. 415–425; doi:10.1007/s002180050422.
9. *Oganessian Yu. Ts. et al.* On the Stability of the Nuclei of Element 108 with  $A = 263-265$  // *Z. Phys. A: Hadrons Nucl.* 1984. V. 319. P. 215–217; doi:10.1007/BF01415635.
10. *Robinson A. P. et al.* Search for a 2-Quasiparticle High- $K$  Isomer in  $^{256}\text{Rf}$  // *Phys. Rev. C.* 2011. V. 83, No. 6. P. 064311; doi:10.1103/PhysRevC.83.064311.

11. *Turchin V.F., Kozlov V.P., Malkevich M.S.* The Use of Mathematical-Statistics Methods in the Solution of Incorrectly Posed Problems // *Sov. Phys. Usp.* 1971. V. 13, No. 6. P. 681–703; doi:10.1070/pu1971v013n06abeh004273.
12. *Turchin V.F.* Solution of the Fredholm Equation of the First Kind in a Statistical Ensemble of Smooth Functions // *USSR Comp. Math. Math. Phys.* 1967. V. 7, No. 6. P. 79–96; doi:10.1016/0041-5553(67)90117-6.
13. *Mukhin R.S. et al.* Reconstruction of Spontaneous Fission Neutron Multiplicity Distribution Spectra by the Statistical Regularization Method // *Phys. Part. Nucl. Lett.* 2021. V. 18, No. 4. P. 439–444; doi:10.1134/S1547477121040130.
14. *Andreev A.V. et al.* Possible Explanation of Fine Structures in Mass–Energy Distribution of Fission Fragments // *Eur. Phys. J. A.* 2004. V. 22, No. 1. P. 51–60; doi:10.1140/epja/i2004-10017-9.
15. *Paşca H. et al.* Simultaneous Description of Charge, Mass, Total Kinetic Energy, and Neutron Multiplicity Distributions in Fission of Th and U Isotopes // *Phys. Rev. C.* 2021. V. 104, No. 1. P. 014604; doi:10.1103/PhysRevC.104.014604.
16. *Isaev A.V. et al.* Prompt Neutron Emission in the Spontaneous Fission of  $^{246}\text{Fm}$  // *Eur. Phys. J. A.* 2022. V. 58, No. 6. P. 108; doi:10.1140/epja/s10050-022-00761-3.
17. *Wild J.F. et al.* Prompt Neutron Emission from the Spontaneous Fission of  $^{260}\text{Md}$  // *Phys. Rev. C.* 1990. V. 41, No. 2. P. 640–646; doi:10.1103/PhysRevC.41.640.
18. *Isaev A.V. et al.* The SFiNx Detector System // *Phys. Part. Nucl. Lett.* 2022. V. 19, No. 1. P. 37–45; doi:10.1134/S154747712201006X.
19. *Hulet E.K. et al.* Spontaneous Fission Properties of  $^{258}\text{Fm}$ ,  $^{259}\text{Md}$ ,  $^{260}\text{Md}$ ,  $^{258}\text{No}$ , and  $^{260}\text{104}$ : Bimodal Fission // *Phys. Rev. C.* 1989. V. 40, No. 2. P. 770–784; doi:10.1103/PhysRevC.40.770.
20. *Mosat P. et al.*  $K$  Isomerism in  $^{255}\text{Rf}$  and Total Kinetic Energy Measurements for Spontaneous Fission of  $^{255,256,258}\text{Rf}$  // *Phys. Rev. C.* 2020. V. 101, No. 3. P. 034310; doi:10.1103/PhysRevC.101.034310.
21. *Carjan N. et al.* Fission of Transactinide Elements Described in Terms of Generalized Cassinian Ovals: Fragment Mass and Total Kinetic Energy Distributions // *Nucl. Phys. A.* 2015. V. 942. P. 97–109; doi:10.1016/j.nuclphysa.2015.07.019.

Received on November 23, 2022.

Редактор *В. В. Булатова*

Подписано в печать 28.07.2022.

Формат 60 × 90/16. Бумага офсетная. Печать офсетная.

Усл. печ. л. 2,0. Уч.-изд. л. 2,81. Тираж 110 экз. Заказ № 60477.

Издательский отдел Объединенного института ядерных исследований  
141980, г. Дубна, Московская обл., ул. Жолио-Кюри, 6.

E-mail: [publish@jinr.ru](mailto:publish@jinr.ru)

[www.jinr.ru/publish/](http://www.jinr.ru/publish/)